ZITA MEDICAL MANAGEMENT

www.hsmc.gr/en/pharmakeftiki-journal/

ΦΑΡΜΑΚΕΥΤΙΚΗ, 38, I, 2026 | 56-65

PHARMAKEFTIKI, 38, I, 2026 | 56-65

ΕΡΕΥΝΗΤΙΚΗ ΕΡΓΑΣΙΑ

RESEARCH AARTICLE

Rational Design, Synthesis, And Enzymatic Evaluation of Spiroquinazoline Derivatives as Promising Acetylcholinesterase Inhibitors

Shuhad Yaseen[1,2], Qais Abualassal[1]*, Zead Abudayeh[1], Amgad Albohy[3]

[1]Department of Applied Pharmaceutical Sciences and Clinical Pharmacy, Faculty of Pharmacy, Isra University, Amman, Jordan

[2]Department of Pharmaceutical Chemistry, Faculty of Pharmacy, College of Pharmacy, University of Al-Nahrain, Baghdad, Iraq

[3]Department of Pharmaceutical Chemistry, Faculty of Pharmacy, The British University in Egypt (BUE), El-Sherouk City, Suez Desert Road, Cairo 11837, Egypt

DOI: https://doi.org/10.60988/p.v38i1.295

ABSTRACT

Spiroquinazoline derivatives represent promising scaffolds for the development of novel anti-Alzheimer's disease (AD) agents. In this study, three quinazoline derivatives (1–3) were synthesized from N-methylisatoic anhydride and fully characterized. Furthermore, we conducted in vitro anticholinesterase assays, molecular docking, and SwissADME predictions for the synthesized compounds. Compounds 1-3 were obtained in good yield, with compound 1 demonstrating potent inhibitory activity against acetylcholinesterase (AChE) (IC_{50} = 7.33 ± 0.18 μM). Thus, these compounds have potential for further development for use in Alzheimer's disease (AD) therapy. Future studies are required to elucidate whether compounds 1-3 have direct effects on Tau aggregation or Aβ production and to investigate their full therapeutic potential in the context of these predominant AD hypotheses.

KEYWORDS: Spiroquinazoline derivatives, Ellman's assay, Cholinesterase inhibitors, Molecular docking, ADME properties

ARTICLE INFO:

Received: November 25, 2025

Revised: December 25, 2025

Accepted: February 2, 2026

Available on line: March 30, 2026

*** CORRESPONDING AUTHOR:**

Qais Abualassal

Email: Qais.abualassal@iu.edu.jo

1. Introduction

Dementia affects over 55 million individuals worldwide, with roughly 60% of those living in low- and middle-income countries according to the World Health Organization (WHO). The most common type of dementia is Alzheimer's disease (AD), which accounts for 65–75% ~~percent~~ of all cases[1]. UK studies estimate that there will be a 57% increase in the number of persons with AD in England and Wales between 2016 and 2040, with more than 1.2 million people with AD by 2040, and the major consequence of this increase is driven by longer life expectancy[2].

AD is a complex, multifactorial disorder and it is still unclear due to the complexity of the human brain; and the deficiency of practical animal models and study tools. Several hypotheses regarding AD have been settled, including cholinergic neuron damage, oxidative stress, amyloid-β (Aβ), Tau, inflammation, etc. Therefore, several efforts have been made to improve anti-AD medications based on these hypotheses[3,4].

Among these, the cholinergic hypothesis remains one of the most widely accepted, proposing deficiency in cholinergic transmission in the brain especially in areas like hippocampus and neocortex. The damage of cholinergic neurons in these areas is a characteristic of the disorder and is believed to cause cognitive impairment and loss of short-term memory that happen in AD[5]. Cholinergic neurotransmission has been involved in many disease states. Because acetylcholine (ACh) has a significant role in cognitive process, the cholinergic system is ~~a significant factor~~ implicated in several forms of dementia, as well as AD. Consequently, the main strategy used for the treatment of AD involves the administration of cholinesterase inhibitors. However, these agents do not decrease the disease progression[4,6].

Oxidative stress is associated with an imbalance between the production of endogenous antioxidants defence and reactive oxygen species (ROS). Excess ROS affects all types of cells and biomolecules, including essential ones for life such as RNA, DNA, unsaturated lipid, protein, and enzymes. Furthermore, oxidative stress is presented as one of the most important causes of neurodegeneration, and the onset and development of the diseases. The brain is highly sensitive to the oxidative stress due to the high-energy request, oxidizable polyunsaturated fatty acid, and scarcity of endogenous antioxidant capacity[7,8]. Therefore, several scientific attempts are directed to utilize antioxidant therapy as a pharmacological approach to either prevent or delay the progress of neurodegeneration caused by oxidative stress.

In 1996, scientists found that dehydroevodiamine hydrochloride (DHED) (Figure 1) a constituent of Evodia rutaecarpa plant, could inhibit AChE in vitro and possess anti-dementia effect in vivo. DHED inhibited AChE in a dose dependent manner approving it is an active anti-cholinesterase component in Evodia rutaecarpine[8]. This molecule had the ability to reverse the scopolamine induced dementia model considerably which was a simple model system of AD that correlate between AD and degree of cholinergic neuron damage. The cognitive improving activity of DHED was because of increasing in ACh level in synapse throughout the inhibition activity of AChE. Anti-amnesic action of DHED was more potent than tacrine, while it had lower potency than tacrine in AChE inhibition because DHED has the ability also to increase cerebral blood flow[9,10]. In another study Li and co-workers reported a series of novel 2-(2- indolyl-)-4(3H) –quinazoline derivates. These compounds were designed and synthesized by removal of a methylene groups in position 7, 8 of rutaecarpine C-ring, with the introducing a terminal side chain, which allowed to obtain compounds with high inhibitory activity against AChE[11].

The aim of this work is to design and synthesize spiroquinazoline derivatives 1-3 by coupling reaction with the antioxidant p-coumaric acid (Scheme 1). Meanwhile, the enzymatic evaluation and molecular modelling of the AChE inhibition for the synthesized quinazoline derivatives are reported.

2. Material and Methods

All reagents were obtained from commercial suppliers and used without any further purification. Acetylthiocholine iodide, Acetylcholinesterase lyophilized powder (electrophorus electricus, electric eel), DTNB {5,5-dithio-bis-(2-nitro benzoic acid)} were purchased from Sigma-Aldrich.

2.1. Ellman's Assay

The AChE activity of the synthesized compounds

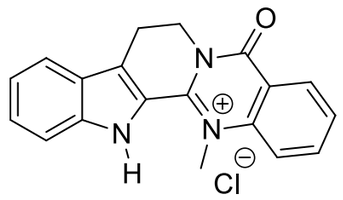

DHED hydrochloride

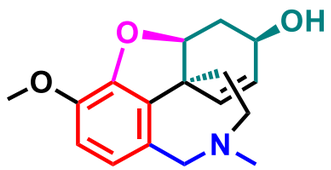

Galantamine

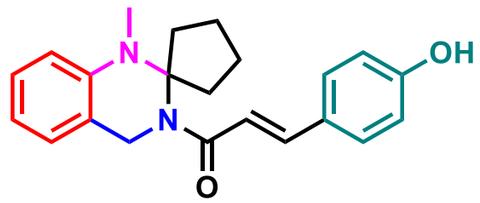

Compound 3

Figure 1. *Top: Structure of DHED hydrochloride. Bottom: Structure of galantamine and test compound **3**.*

(1-3) was tested in vitro utilizing the well-known established spectrophotometric method called Ellman's assay[12]. In this procedure acetylcholine is substituted by acetylthiocholine iodide, followed by the reaction of the thiocholine product with 5,5-dithiobis(2-nitrobenzoic acid) (DTNB, Ellman's reagent) to yield a yellow-coloured anion, 5-thio-2-nitrobenzoic acid (TNB) that is detected spectrophotometrically at 412 nm. A set of test tubes were prepared, each containing 1710 µL of 50 mM Tris–HCl buffer solution pH 7.4 and 20 µL of 10 mM of DTNB. Then, 250 µL of drug sample at different concentrations (25 – 400 µg/mL) and 10 µL of 6.67 UmL^{-1} AChE were added. Galantamine was prepared as a positive control in the same serial concentration of drug sample. All mixture were incubated at 37°C for 15 minutes. Then, 10 µL of 10 mM of acetylthiocholine iodide were added to all samples. Blank samples were prepared with buffer instead of enzyme. The absorbance was measured every 3 seconds for 3 minutes at 412 nm. Acetylcholinesterase Enzyme inhibition (%) was calculated from the rate of absorbance change with time (V= Abs/Δt).

2.2. Chemistry

2.2.1. Synthesis of 2-methylaminobenzamide

This compound was synthesized as previously reported in the literature, and the product was characterized by GC-MS and ^{1}H-NMR spectroscopy [13].

2.2.2. Synthesis of 1'-methyl-1H'-spiro[cyclopentane-1, 2'-quinazolin]-4'(3'H)-one (1)

Compound 1 was synthesized as previously reported in literature utilizing 2-methylaminobenzamide as a starting material, and the product was characterized by GC-MS and ^{1}H-NMR spectroscopy [14].

2.2.3. Synthesis of (E)-3-(4-hydroxyphenyl)-1-(1'-methyl-1'H-spiro [cyclopentane-1,2'- quinazolin]-3'(4'H)-yl) prop-2-en-1-one (3)

To a solution of p-coumaric acid (240 mg, 0.00146 mol) in THF anhydrous, triethylamine (607.2 µL, 0.00437 mol) and thionyl chloride (420 µL, 0.0058 mol) were added, respectively. The solution was stirred for 6 minutes, then a solution of compound 2 (301 mg, 0.00146 mol) in anhydrous THF was added, and the reaction was kept overnight at room temperature. The reaction was quenched with 10 mL of deionized water and then, the reaction mixture was extracted with ethyl acetate and dried over anhydrous $MgSO_4$. The organic layer was combined and concentrated under reduced pressure. The resulting crude product was purified utilizing column chromatography using dichloromethane: methanol (9:1) as mobile phase. The title compound was obtained as white crystals (264 mg, 52% yield).

^{1}H-NMR (300 MHz, $CDCl_3$) δ = 1.75 – 2.0 (m, 8H, cyclopentyl), 3.53 (s, 3H, CH_3), 4.17 (s, 2H, NCH_2), 6.21 (d, 1H, J = 15 Hz, trans-CH=CH), 6.79-6.86 (m, 3H, arom.), 7.19 (s, 1H, arom.), 7.30-7.40 (m, 4H, arom.), 7.55 (d, 1H, J = 15 Hz, trans-CH=CH).

^{13}C-NMR (125 MHz, $CDCl_3$): δ = 26.15, 26.19, 29.22, 29.36, 29.70, 44.54, 115.00, 115.12, 115.26, 115.91, 116.07 (2C), 122.27, 127.09, 129.27, 130.01, 130.38 (2C), 132.28, 144.75, 157.88, 167.55

as shown in Figure 2. MS: m/z = 351.8 $[M+H]^+$, mp 178–181 °C.

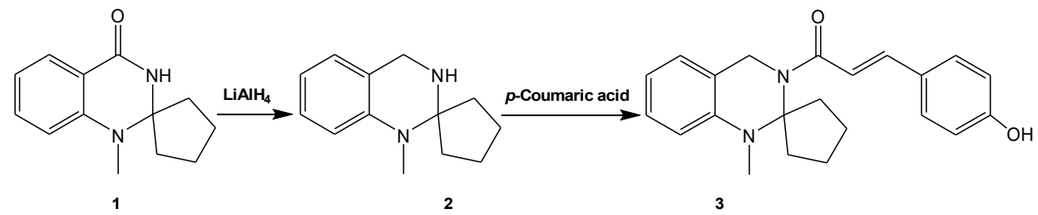

Scheme 1. *Synthesis of compound **3** starting from N-methylisatoic anhydride.*

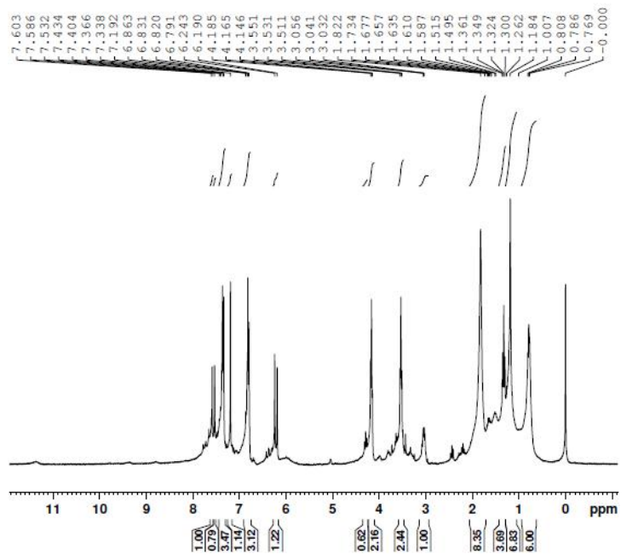

Figure 2*. ^{1}H-NMR spectrum of compound **3**.*

Table 1. Percentage inhibition of AChE activity by compounds **1**-**3** and galantamine at different concentrations.

Compound 1 (µM)	Compound 1 (% Inhibition)	Compound 2 (µM)	Compound 2 (% Inhibition)	Compound 3 (µM)	Compound 3 (% Inhibition)	Galantamine (µM)	Galantamine (% Inhibition)
231.18	97.04 ± 0.088	**247.16**	89.46 ± 0.194	**143.49**	86.16 ± 0.078	**135.77**	97.86 ± 0.180
115.59	91.05 ± 0.288	**123.58**	82.08 ± 0.038	**71.75**	80.06 ± 0.031	**67.88**	95.06 ± 0.092
57.79	83.10 ± 0.108	**61.79**	79.10 ± 0.0150	**35.87**	65.32 ± 0.547	**33.94**	89.99 ± 0.010
28.90	75.74 ± 0.093	**30.89**	70.15 ± 0.042	**17.94**	55.736 ± 0.199	**16.97**	79.51 ± 0.102
14.45	60.49 ± 0.106	**15.45**	50.35 ± 0.191	**8.97**	39.87 ± 0.069	8.49	62.44 ± 0.062

2.2. Molecular Docking

Docking was performed as previously reported[14,15]. The 3D structure of acetylcholinesterase was obtained from the Protein Data Bank (PDB ID: 4EY6).

2.3. ADME Properties

In silico prediction of ADME properties was performed using the SwissADME web server (http://www.swissadme.ch/)[16]. including analyses of gastrointestinal absorption, blood–brain barrier permeability (BOILED-Egg model), and drug-likeness (bioavailability radar).

2.4. Statistical Analysis

Statistical analysis was carried out using Minitab® Version 18 statistical software. For the calculation of Two-way ANOVA, One-way ANOVA and Tukey posttest. Differences were deemed statistically significant at $p \leq 0.05$.

3. Results and Discussion

3.1. Chemical Synthesis and Characterization

Compound 3 was synthesized starting from N-methylisatoic anhydride (Scheme 1), following the procedure previously described by our group[14,17]. In this sequence, reacting 1 with trimethylsilyl chloride (TMSCl), followed by the addition of the powerful reducing agent lithium aluminum hydride ($LiAlH_4$),

Table 2. IC_{50} values (µM) for AChE inhibition by quinazoline derivatives **1**-**3** and galantamine.

Compound	IC_{50} (µM) ± SEM
1	7.33 ± 0.18
2	14.65 ± 0.77
3	18.53 ± 0.92
Galantamine	3.22 ± 0.12

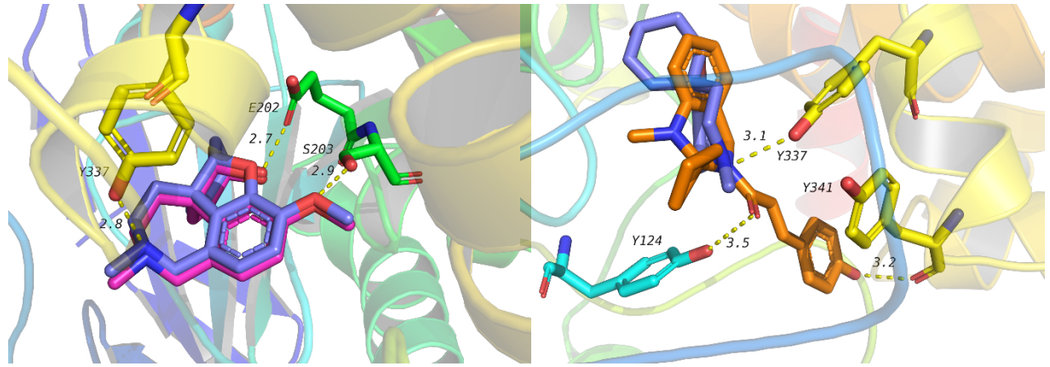

Figure 3. *(a) Validation of docking protocol by re-docking galantamine: the crystallized ligand (blue) shows close overlap with the docked pose (pink). (b) Docking pose of compound 3 (orange) in the active site of AChE, forming polar interactions with residues Y337, Y124, and Y341 (yellow dashed lines), along with hydrophobic contacts within the active-site gorge.*

and afforded compound 2 in excellent yield (90%). Which was subsequently used as an intermediate for the synthesize of compound 3.

Our novel compound 3 was achieved after optimization of the reaction conditions, where the yield of the reaction was enhanced upon increasing the equivalents of thionyl chloride ($SOCl_2$) from 1.5 to 4. The target compound 3 was characterized using ^1H and ^{13}C-NMR spectroscopy, which highlighted the presence of singlet signal at 3.53 ppm is attributed to the N-methyl protons, and the other singlet signal at 4.17 ppm is attributed to N-CH_2 protons. The most diagnostic feature was the presence of two well-resolved doublets at δ 6.21 ppm (J = 15 Hz) and δ 7.55 ppm (J = 15 Hz), where consistent with trans-olefinic protons, confirming the successful coupling of the p-coumaric acid moiety. The ^{13}C-NMR spectrum further demonstrated the propose structure, showing a signal at 167.5 ppm for the conjugated carbonyl carbon. Collectively, these spectral data confirm the successful synthesis of the spiroquinazoline conjugated with p-coumaric acid (compound 3).

3.2. Enzymatic Evaluation

The percentage of inhibition for the three derivatives (1-3) of our quinazoline derivatives against AChE enzyme was performed using Ellman's method to evaluate their inhibitory activity, and the results are shown in Table 1. Compound 1 showed very potent inhibition, at the highest tested concentration (97.041± 0.088%) comparable to galantamine (97.863±0.180) Furthermore,

Table 3. Docking scores (kcal/mol) of galantamine and compound **3** against AChE.

Compound	Docking score (kcal/mol)
3	-10.5
Galantamine	-10.1

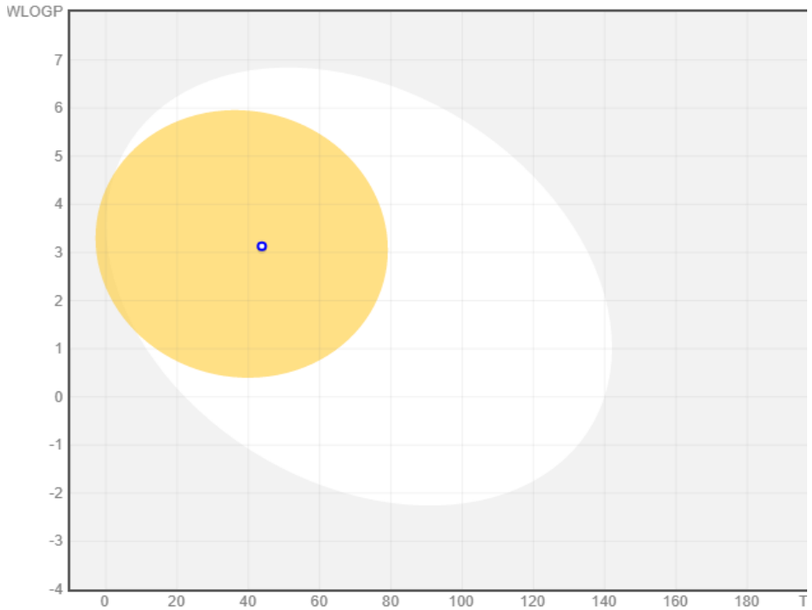

Figure 4. *BOILED-Egg model of compound 3 predicted by SwissADME. The blue circle represents the compound positioned in the yellow region (yolk), indicating high probability of blood–brain barrier (BBB) penetration, as well as good gastrointestinal absorption.*

compounds 2 and 3 demonstrated potent inhibition of AChE (89.46±0.19) and (86.16±0.08), respectively, at their highest tested concentrations. Employing two-way ANOVA analysis revealed that there is a statistically significant difference between products ($p < 0.001$) and their concentration ($p < 0.001$). As expected, increasing concentration resulted in an increase in inhibition while, Galantamine and compound 1 showed superior effect compared with other two compounds. Tukey's posttest showed that there is no statistically significant difference between galantamine and compound 1 at any concentration tested.

The half-maximal inhibitory concentration (IC_{50}) values (Table 2) for the three compounds (1, 2 and 3) indicated that compound 1 was the strongest AChE inhibitor among the synthesized derivatives (IC_{50} = 7.33 µM, comparable to the reference galantamine as presented in Table 2. Overall, there is a significant difference between compounds (one-way ANOVA, $p < 0.001$) with galantamine and 1 showing superior inhibition at lower concentrations, compared with compounds 2 and 3. In addition, on a molar basis, compound 3 exhibited a lower IC_{50} Against AChE (IC_{50} = 18.53 µM) than our previously synthesized ferulic acid derivative (IC_{50} = 31.44 µM)[17].

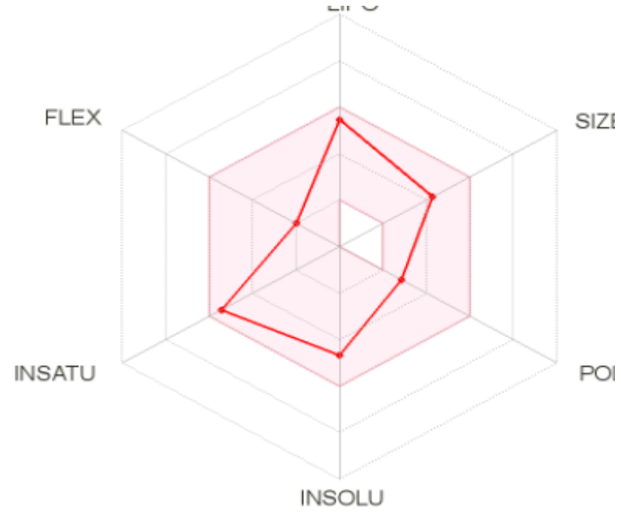

Figure 5. *Bioavailability radar shows that compound **3** has optimum physicochemical properties in terms of drug-likeness.*

3.3. Molecular Docking

Docking of compound 3 in the active site of AChE was used to investigate its potential binding pose. Initially, the docking procedure was validated through the redocking of the co-crystalized ligand, galantamine. The docking software was able to predict the correct pose with high accuracy as seen in Figure 3a. The docked structure was able to maintain all interactions in the crystal structure including interactions with Y337, E202 and S203 (Figure 3b). Other hydrophobic interactions are also maintained with the active site.

The docking score of the co-crystalized ligand was found to be -10.1 kcal/mol (Table 3), which is a comparable binding affinity to galantamine, suggesting favourable binding interactions. supported by its favorable docking score and conserved interactions with key residues.

3.4. ADME properties

The ADME properties of compound 3 were predicted using SwissADME server. The BOILED-Egg diagram as shown in Figure 4 suggests that the compound is orally bioavailable and can cross the blood brain barrier, which is important for compounds targeting Alzheimer's disease.

In addition, the bioavailability radar illustrated in Figure 5 indicates that the physicochemical properties of compound 3 are within acceptable ranges, which suggests drug-like properties and potential suitability for further development.

4. Conclusion

The quinazoline scaffold has emerged as a promising moiety for the design and development of anti-Alzheimer's disease (AD) drugs. Due to its multifaceted pharmacological activities, quinazoline derivatives exhibited significant inhibitory activity against cholinesterase enzymes involved in the

breakdown of acetylcholine, thereby alleviating cholinergic transmission deficits observed in AD. In this work, the design and synthesis of a novel quinazoline derivative compound 3 was achieved from 1-N-methylisatoic anhydride through multiple chemical steps, the final step afforded compound 3 in a good yield (52 %). The synthesized compounds 1-3 were subsequently evaluated in silico through molecular docking studies for cholinesterase inhibitory activity. These findings suggest that spiroquinazoline compounds 1-3 may represent a promising scaffold for the development of new anti-acetylcholinesterase agents.

Acknowledgments

The authors would like to thank Isra University for its financial support of this project.

Funding

This research was financially supported by Isra University.

Conflict of Interest

The authors declare that there is no conflict of interest associated with this work.

References

1. World Health Organization (WHO). Dementia. Geneva, 2019. Available from: https://www.who.int/news-room/fact-sheets/detail/dementia (accessed 1 December 2020).
2. Rasmussen J., and Langerman H. Alzheimer's disease–why we need early diagnosis. *Degener. Neurol. Neuromuscul. Dis.* 24, 123-130, 2019 doi: 10.2147/DNND.S228939
3. Du X., Wang X., and Geng M. Alzheimer's disease hypothesis and related therapies. *Transl. Neurodegener*. 7, 1–7, 2018. doi:10.1186/s40035-018-0107-y
4. Abualassal Q., Abudayeh Z., Sirhan A., and Mkia A. Exploring quinazoline as a scaffold for developing novel therapeutics in Alzheimer's disease. *Molecules* 30, 555, 2025. doi:10.3390/molecules30030555
5. Stanciu G.D., Luca A., Rusu R.N., Bild V., Beschea Chiriac S.I., Solcan C., Bild W., and Ababei D.C. Alzheimer's disease pharmacotherapy in relation to cholinergic system involvement. *Biomolecules* 10, 40, 2019. doi:10.3390/biom10010040
6. Dighe S.N., Tippana M., van Akker S., and Collet T.A. Structure-based scaffold repurposing toward the discovery of novel cholinesterase inhibitors. ACS Omega 5, 30971–30979, 2020. doi:10.1021/acsomega.0c03848
7. Guo C., Sun L., Chen X., and Zhang D. Oxidative stress, mitochondrial damage and neurodegenerative diseases. *Neural Regen. Res.* 8, 2003–2014, 2013. doi:10.3969/j.issn.1673-5374.2013.21.009
8. Cheignon C., Tomas M., Bonnefont-Rousselot D., Faller P., Hureau C., Collin F. Oxidative stress and the amyloid beta peptide in Alzheimer's disease. *Redox Biol*. 14, 450–465, 2018.
9. Park C.H., Kim S.H., Choi W., Lee Y.J., Kim J.S., Kang S.S., Suh Y.H. Novel anticholinesterase and antiamnesic activities of dehydroevodiamine, a constituent of Evodia rutaecarpa. *Planta Med*. 62(5), 405–409, 1996. doi:10.1055/s-2006-957926
10. Wang B., Mai Y.C., Li Y., Hou J.Q., Huang S.L., Ou T.M., Tan J.H., An L.K., Li D., Gu L.Q., Huang Z.S. Synthesis and evaluation of novel rutaecarpine derivatives and related alkaloids derivatives as selective acetylcholinesterase inhibitors. *Eur. J. Med. Chem*. 45(4), 1415–1423, 2010. doi:10.1016/j.ejmech.2009.12.044
11. Li Z., Wang B., Hou J.Q., Huang S.L., Ou T.M., Tan J.H., An L.K., Li D., Gu L.Q., Huang Z.S. 2-(2-indolyl)-4(3H)-quinazolines derivatives as new inhibitors of AChE: design, synthesis, biological evaluation and molecular modelling. *J. Enzyme Inhib. Med. Chem*. 28, 583–592, 2013. doi:10.3109/14756366.2012.663363
11. Ellman G.L., Courtney K.D., Andres V. Jr., Feather-Stone R.M. A new and rapid colorimetric determination of acetylcholinesterase activity. Biochem. Pharmacol. 7(2), 88–95, 1961. doi:10.1016/0006-2952(61)90145-9
12. Abualassal Q., Abudayeh Z., Husein-Al-Ali S.H. Synthesis of a spiroquinazoline compound as potential drug useful in the treatment of Alzheimer's disease. Pharmakeftiki 31(2), 60-68, 2019.
13. Alsuhaimat R., Abualassal Q., Abudayeh Z., Ebada S., Albohy A. Synthesis and docking studies of a novel tetrahydroquinazoline derivative as a promising scaffold for acetylcholinesterase inhibition. Egypt. J. Chem. 63, 4797–4804, 2020.
14. Trott O., Olson A.J. AutoDock Vina: improving the speed and accuracy of docking with a new scoring function, efficient optimization and multithreading. J. Comput. Chem. 31, 455–461, 2010.
15. Daina A., Michielin O., Zoete V. SwissADME: a free web tool to evaluate pharmacokinetics, drug-likeness and medicinal chemistry friendliness of small molecules. Sci. Rep. 7, 42717, 2017.
16. Aleed S., Abualassal Q., Abudayeh Z. Synthesis and biological activities of novel spiroquinazoline derivatives for Alzheimer's disease. Trop. J. Pharm. Res. 23(11), 1879–1885, 2024. doi:10.4314/tjpr.v23i11.11